

# Machine learning based stator-winding fault severity detection in induction motors

Partha Mishra<sup>1</sup>, Shubhasish Sarkar<sup>2</sup>, Sandip Saha Chowdhury<sup>3</sup>, Santanu Das<sup>2</sup>

<sup>1</sup>Department of Electrical Engineering, College of Engineering and Management, Kolaghat, India

<sup>2</sup>Department of Electrical Engineering, Jalpaiguri Government Engineering College, Jalpaiguri, India

<sup>3</sup>Department of Electrical Engineering, Academy of Technology, Hooghly, India

## Article Info

### Article history:

Received Jul 20, 2024

Revised Oct 22, 2024

Accepted Oct 30, 2024

### Keywords:

Discrete wavelet transforms  
Error correcting output codes  
Induction motors  
Statistical feature  
Stator winding faults  
Support vector machine

## ABSTRACT

Approximately 35% of all induction motor defects are caused by stator inter-turn faults. In this paper a novel algorithm has been proposed to analyze the three-phase stator current signals captured from the motor while it is in operation. The suggested method seeks to identify stator inter-turn short circuit faults in early stage and take the appropriate action to prevent the motor's condition from getting worse. Three-phase current signals have been captured under healthy and faulty conditions of the motor. Involving discrete wavelet transform (DWT) based decomposition followed by reconstruction using inverse DWT (IDWT), 50 Hz fundamental component has been removed from the captured raw current signals. Subsequently, from each phase current 15 statistical parameters have been retrieved. The statistical parameters include mean, standard deviation, skewness, kurtosis, peak-to-peak, root mean square (RMS), energy, crest factor, form factor, impulse factor, and margin factor. At the end, a standard machine learning algorithm namely error correcting output codes-support vector machine (ECOC-SVM) has been employed to classify six different severity of stator winding faults. The proposed fault diagnosis method is load and motor-rating independent.

*This is an open access article under the [CC BY-SA](https://creativecommons.org/licenses/by-sa/4.0/) license.*



## Corresponding Author:

Santanu Das

Electrical Engineering Department, Jalpaiguri Government Engineering College

Jalpaiguri, India

Email: santanu.ddas@gmail.com

## 1. INTRODUCTION

Induction motors have a wide application in industries and their failure can lead to significant financial losses. Degradation and failure in turn-insulation in the winding of the stator of a three-phase induction motor are referred to as stator winding faults. If these faults at their early stages are not fixed right away, they may result in performance decline or possibly complete motor failure [1], [2]. An inter-turn short circuit (ITSC) is a typical stator winding fault that happens when two or more turns of same phase or different phases are in direct electrical contact, resulting in an excessive current flow that consequently harm the motor severely [3], [4]. An open circuit is a different kind of fault that results when there is a break or discontinuity in one or more phases of the stator winding. A single phase of the stator winding may also experience inter-turn faults. These issues entail a short circuit between wire turns within the same coil that are adjacent to each other [5]. Over the last few decades; condition monitoring gained more importance as it provides useful information regarding the motor health. It may be classified in two ways namely basic level and advanced level condition monitoring. Basic level condition monitoring has been carried out by measuring the stator current in different fault and load condition, vibration level of rotor. Advanced level monitoring mainly based on fourier transform, wavelet transform, Park's vector method, statistical analysis,

machine learning in combination with fault diagnosis algorithm [6]. Motor current signatures [3], [4], [6], vibration [7], [8], air gap flux [9], acoustic signal [10] of motor are the most significant parameters which are widely used for stator winding fault diagnosis. Several other methods such as insulation resistance testing, polarization index testing, and partial discharge analysis, can also be used to identify stator winding problems [11], [12]. Recently, Almounajjed *et al.* [13] have presented a condition monitoring technique where the accuracy of Motor Current Signature Analysis (MCSA) has been enhanced by introducing discrete wavelet transform (DWT). Stationary wavelet transforms [1], continuous wavelet transform (CWT) [14], reliable flux-based detection [15]-[19], may effectively be used to extract significant features from the signals under analyses. In more advanced schemes of fault diagnosis that are used to increase the performance of fault detection, machine learning methods are incorporated with signal processing tools. Over the years, researchers have proposed several advanced signal processing techniques such as principal component analysis (PCA) [20], independent component analysis (ICA) [21], and zero-sequence component analysis [22]. Statistical measures of the stator current data such as mean, variance, skewness, and kurtosis, may also be used with some modern classifier to identify the motor faults [23], [24]. Recently there has been an increasing interest in deep learning and machine learning techniques for the diagnosis of faults in induction motors [25]-[30]. Deep learning-based networks are more effective than machine learning as they can identify integral features of the original data. Recently, convolutional neural network (CNN) based deep learning has been effectively used in fault diagnosis of electrical machines, biomedical engineering, pattern recognition of images and videos, identification and localization of objects [31]-[37]. However, in case of decision making, few of these algorithms are influenced by many external conditions. Presence of noise during raw data acquisition, different inverter frequencies, harmonics, and efficiency of the data acquisition systems, may lead to erroneous fault detection. In machine learning based researches, it has been found that feature selection, effective feature extraction are exhaustive work and requires expert knowledge. In spite of having all the constraints and limitations, these techniques help to achieve better utilization of equipment in periodic maintenance of the motor. It is quite evident that the regular maintenance including insulation testing, vibration analysis and thermal monitoring can avoid or minimize the possibility of motor failure. This fact trades the need of a non-invasive condition monitoring tool for induction motor in the industries.

After going through a decent literature survey, it may be found that the researchers mostly investigated multiple signals such as current, vibration, thermal, and acoustic, to develop a suitable fault diagnosis method. Moreover, most of the recently proposed fault diagnosis techniques are based on several complex signal processing and classification tools which subsequently require high computation time for execution purpose. But the industries demand fast responding motor condition monitoring technique that can detect the fault within its lead time in order to protect the motor from possible catastrophic failure. Henceforth, the authors of the present work have set the objective of the study as to obtain prudent fault indicators for ITSC faults in stator-winding of induction motor, which takes less computation time. In the process, the authors proposed a simple yet highly efficient motor fault diagnosis technique that involves different statistical features extraction from the three-phase stator current signatures only, and subsequently identification of the class of faults using suitably selected machine learning method. The purpose of the proposed method is to provide a reliable and accurate fault diagnosis and detection technique for stator winding inter-turn faults in induction motors to facilitate the condition-based maintenance (CBM) scheme in order to improve reliability of the production process and reduce maintenance costs.

## 2. SCOPE OF THE WORK

In this work, a simpler but robust and novel fault diagnosis technique based on analysis of three phase stator currents has been proposed. The proposed technique may detect different severity of ITSC faults involving very few numbers of turns (minimum of 0.28% of total turns in a phase winding) in stator winding of the induction motor. Statistical features were used in error correcting output codes-support vector machine (ECOC-SVM) classifier for the early detection of the ITSC faults with a high degree of accuracy. Henceforth, the scope of the work includes:

- Extracting 15 regular statistical features from motor current signals under different operating conditions of the motor namely healthy and 6 different severities of ITSC faults in motor stator winding.
- Implementing an ECOC-SVM machine-learning based algorithm to detect fault classes of varying severity with adequate accuracy.

Entire study has been carried out following the work-flow diagram shown in Figure 1. Upon setting up a customized hardware setup, a series of experiments were performed under different operating conditions of the motor. First, three phase motor current signals were collected. Then, the captured current signals were reconstructed by removing the fundamental frequency (50 Hz) component with the help of DWT and inverse-DWT (IDWT). Statistical feature extractions followed by feeding of the extracted features to ECOC-

SVM machine learning classifier were subsequently performed to classify the different cases under study. 94% classification accuracy could be achieved through the proposed fault diagnosis method.

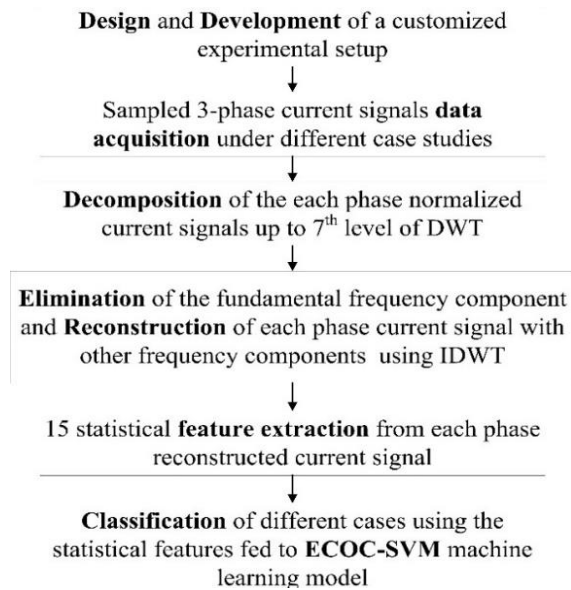


Figure 1. Work flow diagram of the proposed fault diagnosis method

### 3. METHOD

#### 3.1. Arrangement of experimental setup to capture three phase motor current data

The whole experiment has been performed on a 2 hp, 320 V, 3-phase induction motor with customized star connected stator winding. The motor under study contains 6 coils and 360 turns per phase winding. Each of the three-phase winding was customized to implement different inter-turn fault conditions. Tappings from different turns of the customized windings were brought out to a patch board shown in Figure 2 and then were fitted to different terminals to artificially implement ITSC faults of different severity. The 3-phase induction motor was coupled with a DC generator feeding power to a group of lamp loads, to operate the motor at various load conditions. 3 single-phase auto transformers each capable to vary voltage from 0% to 125% were used in between the supply and the motor for keeping the 3-phase supply voltages to balanced condition irrespective of supply voltage fluctuations. A YOKOGAWA make 3-phase digital power meter was interfaced with the motor and a PC, for acquiring three phase motor current signals. A photograph of the experimental setup along with the component markers has been shown in Figure 2.

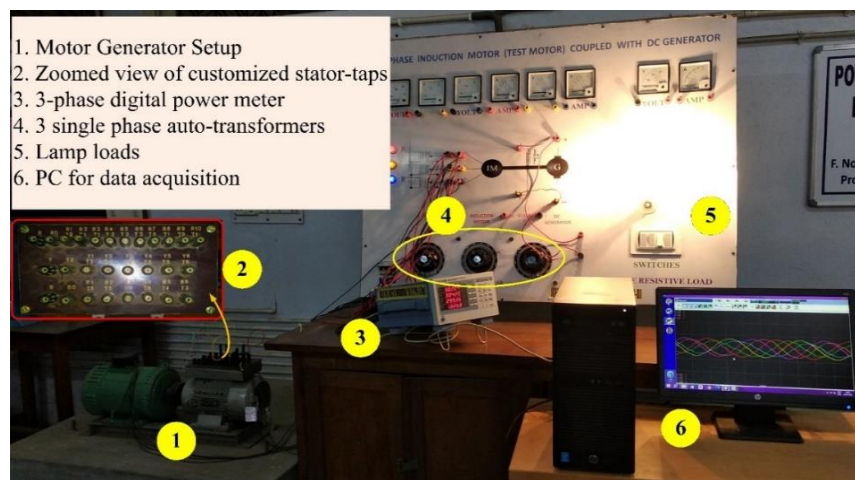


Figure 2. Photograph of the experimental setup

### 3.2. Theoretical background of discrete wavelet transforms

The wavelet transforms, an extension of the short-time fourier transform (STFT) is capable of analyzing a non-stationary signal in both time and frequency domain simultaneously with flexible mathematical substances. CWT and DWT are the two types of wavelets transforms which are frequently used as signal processing tool for fault diagnosis of induction motors [14], [15], [17], [38]-[40]. A brief theoretical background of DWT is discussed as following:

A signal  $x(t)$  is convoluted with a mother wavelet function  $\psi(t)$  to produce the coefficients of CWT as:

$$W_c = \int_{-\infty}^{\infty} x(t)\overline{\psi(t)}dt = \langle x(t), \psi(t) \rangle \tag{1}$$

A time-scale decomposition of the signal  $x(t)$  is obtained by a transformation process in which concept of scale is related to concept of frequency. However, the transformation process involves two parameters i.e. scaling parameter “a” and shifting parameter “b” of the mother wavelet function as (2).

$$\begin{aligned} \psi_a(t) &= \frac{1}{\sqrt{|a|}}\psi\left(\frac{t}{a}\right) \\ \psi_{a,b}(t) &= \frac{1}{\sqrt{|a|}}\psi\left(\frac{t-b}{a}\right) \end{aligned} \tag{2}$$

Therefore, the process defined by (1) is converted to the process defined by (3).

$$\begin{aligned} W_{C\psi_{ab}} &= \int_{-\infty}^{\infty} x(t)\overline{\psi_{ab}(t)}dt = \langle x(t), \psi_{ab}(t) \rangle \\ W_{C_{a,b}} &= \frac{1}{\sqrt{|a|}}\int_{-\infty}^{\infty} x(t)\overline{\psi\left(\frac{t-b}{a}\right)}dt \end{aligned} \tag{3}$$

The DWT is derived through sampling the scaling and shifting parameters of CWT as shown in (4), which is also known as dyadic discretization method where the parameters time (t), scale (a) and shifting (b) are considered in their discrete versions n, j and k, respectively. However, the continuous variables a and b are converted into discrete variables in form of  $a=2^j$  and  $b=k2^j$ , where  $j \in \mathbb{N}$  and  $k \in \mathbb{Z}$  [15].

$$\psi_{(j,k)}(n) = \frac{1}{\sqrt{2^j}}\psi\left(\frac{n-2^j k}{2^j}\right) \tag{4}$$

Therefore, the continuous wavelet process described in (3) is converted into discrete wavelet process as (5).

$$\begin{aligned} W_{C\psi_{j,k}} &= \sum_n x(n)\overline{\psi_{j,k}(n)} \\ W_{C_{j,k}} &= \sum_n x(n)\overline{\psi_j(n - 2^j k)} \end{aligned} \tag{5}$$

The DWT of a signal is implemented by following the guidelines of Mallat algorithm in which a bandpass filter bank is used [17]. According to the principle of Mallat algorithm, in the first level of decomposition, bandwidth of the original signal is halved after passing through a low pass and a high pass filter. In this process, the original signal is decomposed into two signals known as low pass approximate coefficients ( $AC_1$ ) and high pass detail coefficients ( $DC_1$ ). Then,  $AC_1$  is decomposed into signals of approximate coefficients and detail coefficients at level 2 i.e.  $AC_2$  and  $DC_2$  by passing  $AC_1$  through the same decomposition process as discussed above. However, the higher-level coefficients are obtained through further application of the decomposition process on approximate coefficient signals of corresponding level. But the maximum level of decomposition is restricted to the sample length of the original signal because in each decomposition level, the sample length gets reduced to half of the input sample size. From (6), it can be observed that overall bandwidth of the signal under transformation is divided in exact powers of two along time. However, as per Nyquist theorem, bandwidth of the signal is less than or equal to half the sampling frequency ( $f_s$ ). Therefore, bandwidth of the approximate and detail coefficients at an analysis level L can be related to the sampling frequency ( $f_s$ ) as shown in (6).

$$AC_L \Rightarrow \left[0, \frac{f_s}{2^{L+1}}\right] \quad \text{and} \quad DC_L \Rightarrow \left[\frac{f_s}{2^{L+1}}, \frac{f_s}{2^L}\right] \tag{6}$$

**3.3. Formulation of statistical features**

A set of quantified statistical values depicting the characteristics of the time series data was extracted from the reconstructed signals, and later was used as significant features for the fault’s classification purpose. In the current study, 15 conventional statistical features were extracted from the three-phase reconstructed current signals. The mathematical formulae of the used statistical features have been listed in Table 1. Let,  $x_i$  is the  $i^{\text{th}}$  data sample of a single-cycle-single-phase current vector ( $x$ ) consisting  $N$  number of data samples, and  $i=1, 2, 3, \dots, N$ .

Table 1. Mathematical formulae of used statistical feature

Sl no	Statistical parameter	Mathematical formulae	Sl no	Statistical parameter	Mathematical formulae
1	Mean	$\mu = \frac{1}{N} \sum_{i=1}^N x_i$	9	Crest factor	$CF = \frac{x_p}{x_{rms}}$
2	Maximum value	Max(x)	10	Latitude factors	$LF = \frac{x_p}{x_{srm}}$
3	Root mean square (RMS)	$x_{rms} = \sqrt{\frac{1}{N} \sum_{i=1}^N x_i^2}$	11	Impulse Factor	$IF = \frac{x_p}{\frac{1}{N} \sum_{i=1}^N  x_i }$
4	Square root mean (SRM)	$x_{srm} = \frac{1}{N} \sum_{i=1}^N x_i^2$	12	Skewness	$SK = \frac{E(x - \mu)^3}{\sigma^3}$
5	Standard deviation	$\sigma = \sqrt{\frac{1}{N} \sum_{i=1}^N (x_i - \mu)^2}$	13	Kurtosis	$Kurt = \frac{E(x - \mu)^4}{\sigma^4}$
6	Variance	$\sigma^2 = \frac{1}{N} \sum_{i=1}^N (x_i - \mu)^2$	14	Fifth moment	$FM = \frac{E(x - \mu)^5}{\sigma^5}$
7	Shape factor	$SF = \frac{x_{rms}}{\frac{1}{N} \sum_{i=1}^N  x_i }$	15	Sixth moment	$SM = \frac{E(x - \mu)^6}{\sigma^6}$
8	SRM shape factor (SRMSF)	$SF_{SRM} = \frac{x_{srm}}{\frac{1}{N} \sum_{i=1}^N  x_i }$			

**3.4. Theoretical background of ECOC-SVM**

For two-class (binary) classification problems, machine learning techniques namely logistic regression and SVM, are widely used [41]. However, most of the real-life problems are multi-class problems. Currently, a multi-class classification problem is performed by segmenting the problem into a number of binary problems followed by integration of these binary problems. ECOC [42] is one of such methods which are extensively used for multi-class classification problems. In this approach, a  $k$ -class classification problem is converted into a larger number ( $L$ ) of 2-class problems. A unique code word is assigned to each class instead of a class label which is used in other conventional machine learning algorithms. An ECOC that is  $L$  bit long has unique code words,  $C$  and Hamming distance,  $d$ . In general, ECOC is a coding matrix whose elements are 0 and 1. Rows of the matrix represent the class number ( $q$ ) of the samples and columns represent the number of classifiers ( $s$ ) to be trained. In training phase of ECOC, any element of the coding matrix,  $M_{qs}$  equals 1 indicates that the corresponding sample is positive for  $q$ -th class and  $s$ -th classifier. And,  $M_{qs}$  equals 0 indicates that the sample is negative for  $q$ -th class and  $s$ -th classifier. All the classifiers  $f(x)=(f_1(x), f_2(x), \dots, f_s(x))$  are trained according to this principle. To classify a new sample  $X$ , first, the distances between output and class vectors are measured. Then, class with minimum distance is considered to be the classification result which is obtained as (7).

$$Z = \underset{q=[1,2,\dots,Q]}{\text{arg min}} (d(M_q, f(X))) \tag{7}$$

Where,  $Z$  is the class of  $X$  and  $d$  is the Hamming distance which is calculated as (8).

$$d(M_q, f(x)) = \sum_{s=1}^S \frac{|2M_{qs} - \text{sgn}(f_s) - 1|}{2} \tag{8}$$

The length,  $L$  is decided by the method used for generating error-correcting codes. Over the years, various methods like Hadamard-matrix codes, BCH codes, random codes, exhaustive codes, continuous coding, and expectation maximization coding, are proposed. For a  $k$ -class problem,  $L$  must follow  $\log_2 k < L \leq 2^{k-1} - 1$ .

In the present work, the multiclass classification problem has been carried out by the ECOC-SVM classifier that uses combination of ECOC and multiple binary SVM learners. The upper limit of the generalization error for ECOC-SVM has been reported as:

$$\frac{130R^3}{m} (D \log_2(4em) \log_2(16m) + \log_2 \frac{2(2m)^M MNC!}{\delta}) \tag{9}$$

where,

N: number of codes with coding length L and HD between codes

D:  $\sum_{i=1}^L \frac{1}{\gamma_i^2}$

R: minimum radius of enclosure ball

M:  $L - \frac{d-1}{2}$

C: Number of code words of each group

While deriving this upper limit of error it was assumed that  $m$  samples would be suitably classified by  $k$ -class ECOC SVMs with probability at least  $1 - \delta$ . The arranged SVM classification intervals have been represented by  $\gamma_1, \gamma_2, \dots, \gamma_L$ . It is to be noted that with fixed  $L$  and  $d$ , there exists an optimal allocation order for code words that promises best generalization ability of the ECOC-SVM.

#### 4. RESULTS AND DISCUSSION

##### 4.1. Data acquisition and preprocessing of the current signals

Upon development of the customized hardware setup, a series of experiments were conducted to capture 3-phase line currents under different operating conditions of the motor. All the experiments were carried out at balanced 3-phase supply voltage with  $\pm 0.5\%$  tolerance limit. Data acquisition were carried out for healthy and 6 different aforementioned ITSC fault conditions by connecting at a time only one short-circuiting link between two taps involving 1, 2, 3, 4, 5, and 6 turns (T1, T2, ..., T6) in R-phase windings of stator. Five different load levels i.e. no-load, 25%, 50%, 75%, and 100% of full load could be achieved, and they have been represented as 0L, 1L, 2L, 3L, and 4L, respectively, in the subsequent sections of the manuscript. All the case-studies along with their identifiers have been listed in Table 2.

Table 2. Case studies along with their identifiers

	Healthy	T1	T2	T3	T4	T5	T6
0L	H_0L	T1_0L	T2_0L	T3_0L	T4_0L	T5_0L	T6_0L
1L	H_1L	T1_1L	T2_1L	T3_1L	T4_1L	T5_1L	T6_1L
2L	H_2L	T1_2L	T2_2L	T3_2L	T4_2L	T5_2L	T6_2L
3L	H_3L	T1_3L	T2_3L	T3_3L	T4_3L	T5_3L	T6_3L
4L	H_4L	T1_4L	T2_4L	T3_4L	T4_4L	T5_4L	T6_4L

At the initial stage of current data collection, multiple observations were repeated corresponding to each operating condition in order to rule out any possibilities of misleading the proposed algorithm due to superfluous effect of noise and momentary problems in data acquisition process. Motor line currents were captured at 20 kHz sampling rate, deploying 3-phase digital power meter which is capable to display RMS values of the signals along with the provision to capture corresponding signals at a given sampling frequency. After capturing current data at all experimental conditions, the current signals were normalized with respect to the peak value of corresponding phase currents obtained at H\_0L condition. Later, one complete cycle comprising approximately 400 sampled data points for each of the normalized three-phase current signals were selected and were considered for further data analysis process. Few exemplary waveforms of three phase currents have been shown in Figure 3, waveforms obtained at H\_0L and 6T\_0L have been presented in Figures 3(a) and 3(b), respectively. It may be observed that due to appearance of fault in stator windings, the motor current signatures distort from usual sinusoidal shapes. However, these changes are difficult to figure out in open eyes when operating condition changes from healthy or some fault level to other fault condition involving nominal number of turns available in the scope of the present study.

##### 4.2. Reconstruction of raw 3-phase current data using DWT and inverse-DWT

It is quite evident that if fault occurs, the three-phase currents become unbalanced. Merely by visually inspecting the graphs of the current signals, it is difficult to differentiate between faulty and healthy cases. Thus, additional analysis of current signals is required to detect the faults accurately. First, the 50 Hz frequency (fundamental frequency) components of the three phase current signals were eliminated because

they do not have any role to play in detecting fault condition of the motor [3]. In this process captured signals sampled at 20 kHz frequency have been decomposed up to seven levels using DWT which is a multi-resolution signal analysis tool. Then, reconstruction of the same signal without 50 Hz frequency component has been implemented using IDWT. Debauches wavelet-2 (Db2 in MATLAB) has been used as mother wavelet in DWT. Exemplary reconstructed R, Y, and B-phase current signals have been plotted and shown in Figure 4. Figure 4(a) represents the reconstructed waveform of R-phase currents obtained at H\_OL, 2T\_OL and 4T\_OL conditions, where as Figures 4(b) and 4(c) represent the Y and B-phase reconstructed waveforms of the same conditions. Significant changes in magnitude and shape of the reconstructed phase current waveforms may be noted due to fault conditions. Thus, the reconstructed signals may carry potential information related to fault or operating condition of the motor.

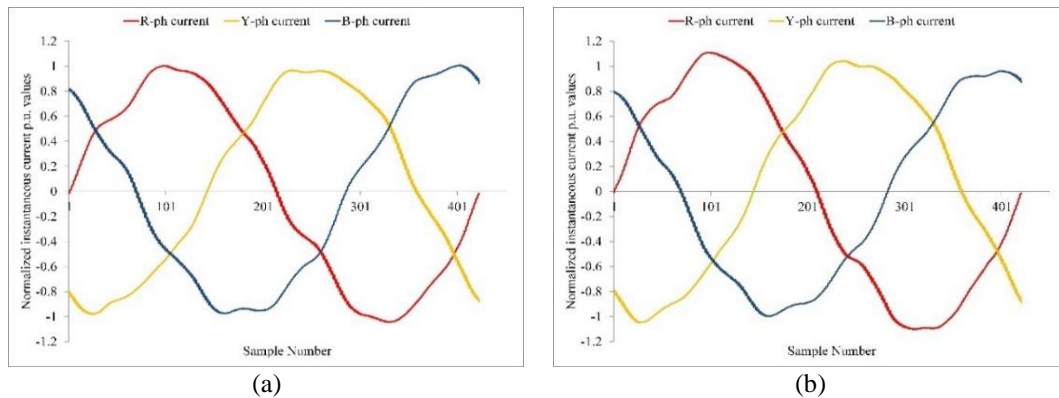


Figure 3. 3-phase current waveforms at (a) H\_OL condition and (b) 6T\_OL condition

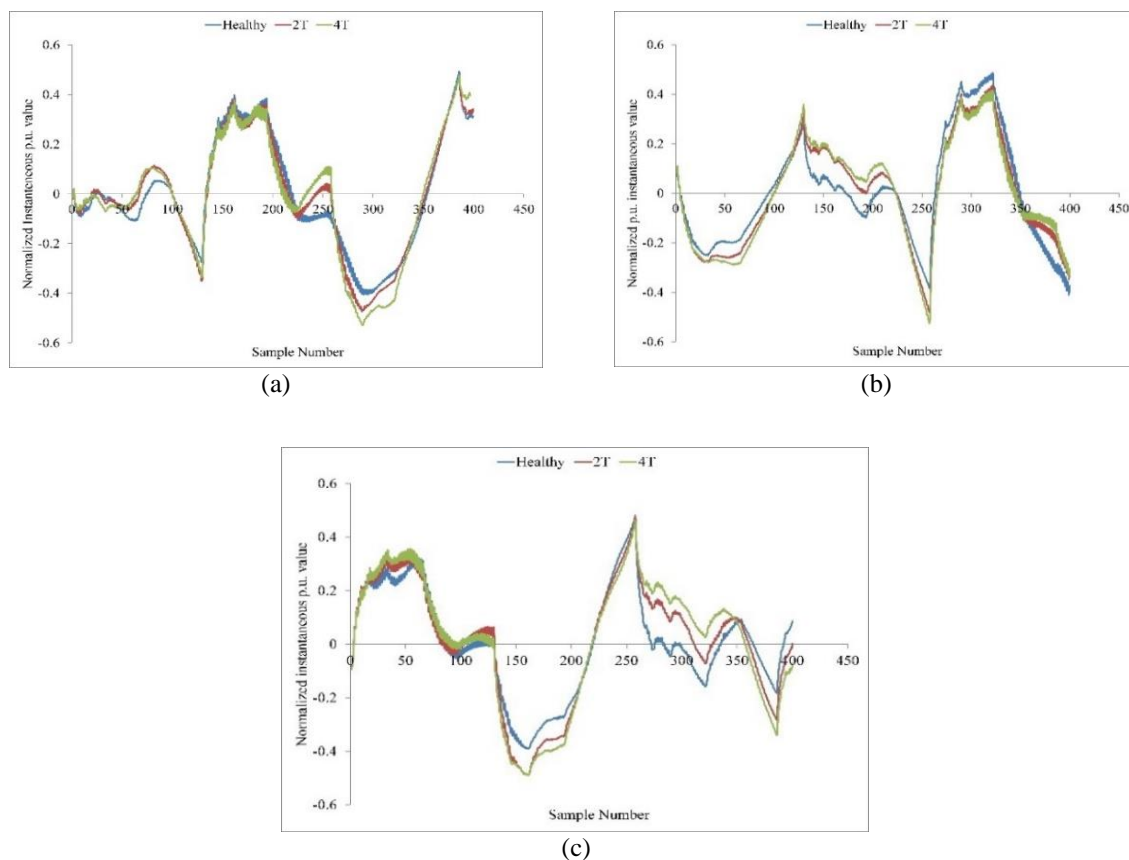


Figure 4. Reconstructed: (a) R-phase, (b) Y-phase, and (c) B-phase current waveforms obtained at H\_OL, 2T\_OL and 4T\_OL conditions

**4.3. Statistical feature extraction**

In the current study, 15 conventional statistical features were extracted from each of the three-phase reconstructed current signals. In total 45 features were extracted. Most of these features were found to have reasonable variance with change of the operating conditions from healthy to highest possible fault condition under the scope of the present study. Change in motor load has also introduced significant effect on the feature values. Variations of few exemplary features at different motor operating conditions have been presented in Figure 5. Figure 5(a) shows the bar plot of mean ( $\mu$ ) values of R-phase reconstructed currents under different operating condition of the motor, and it may be observed that the value of the respective  $\mu$  does not coincide much with varying level of fault under different load conditions. Figure 5(b) represents bar plot of shape factor ( $sf$ ) values extracted from Y-phase reconstructed current. Significant variation of the  $sf$  values could be observed corresponding to varying operating conditions of the motor under different load conditions. So,  $sf$  may be considered as a potential feature for the detection of the faults. However, a definite pattern in change of the  $sf$  values could not be derived. Figure 5(c) represents bar plot of kurtosis ( $kurt$ ) values extracted from B-phase reconstructed current signals. The feature,  $kurt$  seems to be as good as  $sf$ , and was considered as an important feature. After a close observation on all extracted features, it could be noted that all the features are pertinent and include information about the operating condition of the motor. Besides, a large feature set facilitates machine learning algorithm to be trained effectively to make it more robust.

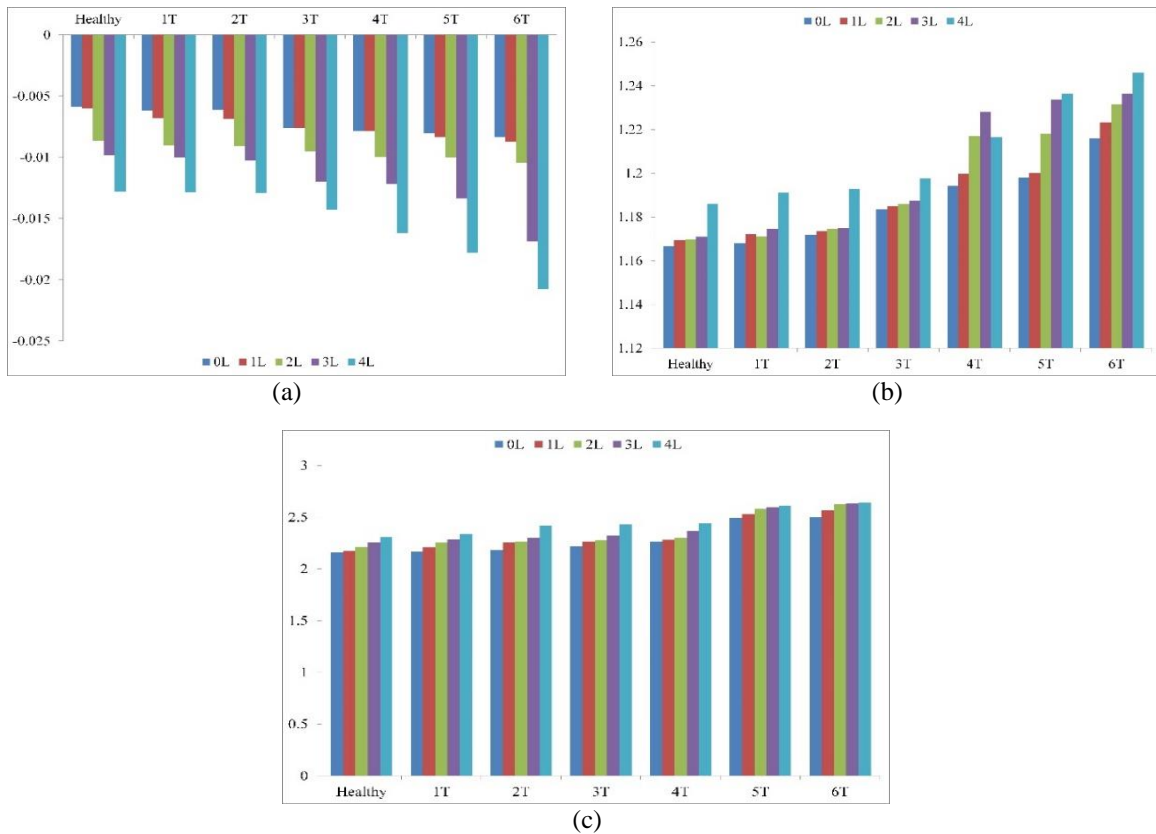


Figure 5. Bar plots of statistical features obtained at different case studies e.g.: (a)  $\mu$  values of R-phase reconstructed currents, (b)  $sf$  values of Y-phase reconstructed currents, and (c)  $kurt$  values of B-phase reconstructed currents different case studies

**4.4. Classification of faults using ECOC-SVM classifier**

Extracted statistical features were used to model the machine learning algorithm involving ECOC aided by SVM, implemented in MATLAB platform. 7 operating cases mentioned in section 4.1, were considered in this study. Each operating case was carried out at five different loading conditions. Each experiment was repeated 4 times. Hence, in total there were  $(7 \times 5 \times 4 = 140)$  140 observations. All the 140 observations were used for training and testing phases of ECOC-SVM classifier. Out of that, 70% of observations were taken for training, and 30% of observations were used for testing purposes. During testing phase, the trained model exhibited reasonably good fault detection accuracy. The result obtained from the



proposed classifier model has been presented in form of a confusion matrix [3], shown in Figure 6. Here, in the confusion matrix, the correct classifications have been shown by blue boxes, and the miss-classifications are shown by pink boxes. It may be noted that approximately 94% classification accuracy could be achieved.

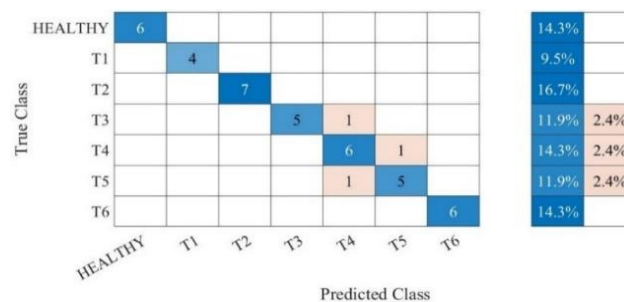


Figure 6. Confusion matrix obtained from testing phase of ECOC-SVM

## 5. CONCLUSION

Detection of minor staged varying severity of ITSC faults at varying loads has always been a tough task. However, the findings of the current study have successfully established a computationally simple yet highly accurate fault-diagnosis method for the early detection of different severity of ITSC faults in a particular phase of motor stator winding. The ability of the proposed technique to accurately detect ITSC faults involving very few numbers of turns, i.e., minimum 0.28% of total turns in a phase winding, makes it unique. The proposed method also established the detection of ITSC faults under varying load levels which makes the fault diagnosis technique load independent. Moreover, normalization of the 3-phase currents at the initial stage of the analyses makes the extracted statistical features machine independent which in-turn ensures the acceptability of the proposed method in condition monitoring of industry-graded 3-phase induction motors. Most importantly, the achieved 94% classification accuracy by the proposed method while classifying different severity of ITSC faults is highly satisfactory. Hence, all these facts strengthen the acceptability of the proposed technique in fault diagnosis of induction motors with different ratings even under different stresses in industrial environment. However, the current study may be expanded by considering varying severity of inter-turn short circuit faults with unbalanced supply voltage and also for the partial insulation faults which provide identical motor line currents obtained in case of ITSC faults. The proposed research work may also be extended to identify the severity of multiple faults that may occur simultaneously in induction motor.

## ACKNOWLEDGEMENTS

The authors would like to acknowledge DST-SERB (grant number: SB/S3/EECE/0172/2013) and AICTE-MODROB (grant number: F.NO:9-25/RIFD/MODROB/Policy-1/2017-18) for funding the current study.

## REFERENCES





- [1] L. Wei, X. Rong, H. Wang, S. Yu, and Y. Zhang, "Method for identifying stator and rotor faults of induction motors based on machine vision," *Mathematical Problems in Engineering*, vol. 2021, pp. 1–13, Jan. 2021, doi: 10.1155/2021/6658648.
- [2] G. S. Ayyappan, B. R. Babu, M. R. Raghavan, and R. Poonthalir, "Genetic algorithm & fuzzy logic-based condition monitoring of induction motor through estimated motor losses," *IETE Journal of Research*, vol. 69, no. 6, pp. 3750–3761, Aug. 2023, doi: 10.1080/03772063.2021.1913075.
- [3] S. Sarkar, P. Purkait, and S. Das, "NI CompactRIO-based methodology for online detection of stator winding inter-turn insulation faults in 3-phase induction motors," *Measurement*, vol. 182, p. 109682, Sep. 2021, doi: 10.1016/j.measurement.2021.109682.
- [4] S. Das, P. Purkait, D. Dey, and S. Chakravorti, "Monitoring of inter-turn insulation failure in induction motor using advanced signal and data processing tools," *IEEE Transactions on Dielectrics and Electrical Insulation*, vol. 18, no. 5, pp. 1599–1608, Oct. 2011, doi: 10.1109/TDEI.2011.6032830.
- [5] G. S. Ayyappan, B. R. Babu, K. Srinivas, M. R. Raghavan, and R. Poonthalir, "Mathematical modelling and IoT enabled instrumentation for simulation & emulation of induction motor faults," *IETE Journal of Research*, vol. 69, no. 4, pp. 1829–1841, May 2023, doi: 10.1080/03772063.2021.1875272.
- [6] M. Z. Ali, M. N. S. K. Shabbir, X. Liang, Y. Zhang, and T. Hu, "Machine learning-based fault diagnosis for single- and multi-faults in induction motors using measured stator currents and vibration signals," *IEEE Transactions on Industry Applications*, vol. 55, no. 3, pp. 2378–2391, May 2019, doi: 10.1109/TIA.2019.2895797.

- [7] S. Yadav, R. K. Patel, and V. P. Singh, "Multiclass fault classification of an induction motor bearing vibration data using wavelet packet transform features and artificial intelligence," *Journal of Vibration Engineering & Technologies*, vol. 11, no. 7, pp. 3093–3108, Oct. 2023, doi: 10.1007/s42417-022-00733-3.
- [8] M. Ojaghi, M. Sabouri, and J. Faiz, "Analytic model for induction motors under localized bearing faults," *IEEE Transactions on Energy Conversion*, vol. 33, no. 2, pp. 617–626, Jun. 2018, doi: 10.1109/TEC.2017.2758382.
- [9] A. Glowacz, W. Glowacz, Z. Glowacz, and J. Kozik, "Early fault diagnosis of bearing and stator faults of the single-phase induction motor using acoustic signals," *Measurement*, vol. 113, pp. 1–9, Jan. 2018, doi: 10.1016/j.measurement.2017.08.036.
- [10] S. Mitra and C. Koley, "Early and intelligent bearing fault detection using adaptive superlets," *IEEE Sensors Journal*, vol. 23, no. 7, pp. 7992–8000, Apr. 2023, doi: 10.1109/JSEN.2023.3245186.
- [11] S. K. Gundewar and P. V. Kane, "Bearing fault diagnosis using time segmented Fourier synchrosqueezed transform images and convolution neural network," *Measurement*, vol. 203, p. 111855, Nov. 2022, doi: 10.1016/j.measurement.2022.111855.
- [12] G. H. Bazan, P. R. Scalassara, W. Endo, and A. Goedel, "Information theoretical measurements from induction motors under several load and voltage conditions for bearing faults classification," *IEEE Transactions on Industrial Informatics*, vol. 16, no. 6, pp. 3640–3650, Jun. 2020, doi: 10.1109/TII.2019.2939678.
- [13] A. Almounajjed, A. K. Sahoo, and M. K. Kumar, "Diagnosis of stator fault severity in induction motor based on discrete wavelet analysis," *Measurement*, vol. 182, p. 109780, Sep. 2021, doi: 10.1016/j.measurement.2021.109780.
- [14] V. B. Bal, N. F. Kotelenets, and M. Deeb, "Discrete wavelet transform for stator fault detection in an induction motor," *Power Technology and Engineering*, vol. 57, no. 1, pp. 175–185, May 2023, doi: 10.1007/s10749-023-01639-0.
- [15] S. Chikkam and S. Singh, "Condition monitoring and fault diagnosis of induction motor using DWT and ANN," *Arabian Journal for Science and Engineering*, vol. 48, no. 5, pp. 6237–6252, May 2023, doi: 10.1007/s13369-022-07294-3.
- [16] H. Talhaoui, T. Ameid, O. Aissa, and A. Kessal, "Wavelet packet and fuzzy logic theory for automatic fault detection in induction motor," *Soft Computing*, vol. 26, no. 21, pp. 11935–11949, Nov. 2022, doi: 10.1007/s00500-022-07028-5.
- [17] G. R. Agah, A. Rahideh, H. Khodadadzadeh, S. M. Khoshnazar, and S. Hedayatikia, "Broken rotor bar and rotor eccentricity fault detection in induction motors using a combination of discrete wavelet transform and Teager-Kaiser energy operator," *IEEE Transactions on Energy Conversion*, vol. 37, no. 3, pp. 2199–2206, 2022, doi: 10.1109/TEC.2022.3162394.
- [18] Y. Park, H. Choi, S. B. Lee, and K. N. Gyftakis, "Search Coil-based detection of nonadjacent rotor bar damage in Squirrel Cage induction motors," *IEEE Transactions on Industry Applications*, vol. 56, no. 5, pp. 4748–4757, Sep. 2020, doi: 10.1109/TIA.2020.3000461.
- [19] S. B. Lee, J. Shin, Y. Park, H. Kim, and J. Kim, "Reliable Flux-based detection of induction motor rotor faults from the fifth rotor rotational frequency sideband," *IEEE Transactions on Industrial Electronics*, vol. 68, no. 9, pp. 7874–7883, Sep. 2021, doi: 10.1109/TIE.2020.3016241.
- [20] S. Marmouch, T. Aroui, and Y. Koubaa, "Induction machine faults diagnosis by statistical neural networks with selection variables based on principal component analysis," in *2017 18th International Conference on Sciences and Techniques of Automatic Control and Computer Engineering (STA)*, Dec. 2017, pp. 99–103, doi: 10.1109/STA.2017.8314887.
- [21] B. Brusamarello, J. C. C. Silva, K. M. Sousa, and G. A. Guarneri, "Bearing fault detection in three-phase induction motors using support vector machine and fiber bragg grating," *IEEE Sensors Journal*, vol. 23, no. 5, pp. 4413–4421, Mar. 2023, doi: 10.1109/JSEN.2022.3167632.
- [22] A. Abid, M. T. Khan, and C. W. de Silva, "Layered and real-valued negative selection algorithm for fault detection," *IEEE Systems Journal*, vol. 12, no. 3, pp. 2960–2969, Sep. 2018, doi: 10.1109/JSYST.2017.2753851.
- [23] H. Khwaja, S. Gupta, and V. Kumar, "A statistical approach for fault diagnosis in electrical machines," *IETE Journal of Research*, vol. 56, no. 3, p. 146, 2010, doi: 10.4103/0377-2063.67099.
- [24] G. Pontuale, F. A. Farrelly, A. Petri, and L. Pitolli, "A statistical analysis of acoustic emission signals for tool condition monitoring (TCM)," *Acoustics Research Letters Online*, vol. 4, no. 1, pp. 13–18, Jan. 2003, doi: 10.1121/1.1532370.
- [25] M. H. Abidi, M. K. Mohammed, and H. Alkhalefah, "Predictive maintenance planning for industry 4.0 using machine learning for sustainable manufacturing," *Sustainability*, vol. 14, no. 6, p. 3387, Mar. 2022, doi: 10.3390/su14063387.
- [26] S. Arena, E. Florian, I. Zennaro, P. F. Orrù, and F. Sgarbossa, "A novel decision support system for managing predictive maintenance strategies based on machine learning approaches," *Safety Science*, vol. 146, p. 105529, Feb. 2022, doi: 10.1016/j.ssci.2021.105529.
- [27] S. Aziz, M. U. Khan, M. Faraz, and G. A. Montes, "Intelligent bearing faults diagnosis featuring automated relative energy based empirical mode decomposition and novel cepstral autoregressive features," *Measurement*, vol. 216, p. 112871, Jul. 2023, doi: 10.1016/j.measurement.2023.112871.
- [28] M. Cakir, M. A. Guvenc, and S. Mistikoglu, "The experimental application of popular machine learning algorithms on predictive maintenance and the design of IIoT based condition monitoring system," *Computers & Industrial Engineering*, vol. 151, p. 106948, Jan. 2021, doi: 10.1016/j.cie.2020.106948.
- [29] P. Kumar and A. S. Hati, "Review on machine learning algorithm based fault detection in induction motors," *Archives of Computational Methods in Engineering*, vol. 28, no. 3, pp. 1929–1940, May 2021, doi: 10.1007/s11831-020-09446-w.
- [30] A. Choudhary, D. Goyal, and S. S. Letha, "Infrared thermography-based fault diagnosis of induction motor bearings using machine learning," *IEEE Sensors Journal*, vol. 21, no. 2, pp. 1727–1734, Jan. 2021, doi: 10.1109/JSEN.2020.3015868.
- [31] Z. Chen, A. Mauricio, W. Li, and K. Gryllias, "A deep learning method for bearing fault diagnosis based on cyclic spectral coherence and convolutional neural networks," *Mechanical Systems and Signal Processing*, vol. 140, p. 106683, Jun. 2020, doi: 10.1016/j.ymssp.2020.106683.
- [32] S. Qi, J. Yang, and Z. Zhong, "A review on industrial surface defect detection based on deep learning technology," in *2020 The 3rd International Conference on Machine Learning and Machine Intelligence*, Sep. 2020, pp. 24–30, doi: 10.1145/3426826.3426832.
- [33] J. J. Saucedo-Dorantes, A. Y. Jaen-Cuellar, M. Delgado-Prieto, R. de J. Romero-Troncoso, and R. A. Osornio-Rios, "Condition monitoring strategy based on an optimized selection of high-dimensional set of hybrid features to diagnose and detect multiple and combined faults in an induction motor," *Measurement*, vol. 178, p. 109404, Jun. 2021, doi: 10.1016/j.measurement.2021.109404.
- [34] D. Dey, B. Chatterjee, S. Dalai, S. Munshi, and S. Chakravorti, "A deep learning framework using convolution neural network for classification of impulse fault patterns in transformers with increased accuracy," *IEEE Transactions on Dielectrics and Electrical Insulation*, vol. 24, no. 6, pp. 3894–3897, Dec. 2017, doi: 10.1109/TDEL.2017.006793.
- [35] B. Ganguly, S. Biswas, S. Ghosh, S. Maiti, and S. Bodhak, "A deep learning framework for eye melanoma detection employing convolutional neural network," in *2019 International Conference on Computer, Electrical & Communication Engineering (ICCECE)*, Jan. 2019, pp. 1–4, doi: 10.1109/ICCECE44727.2019.9001858.





- [36] T. Khan, P. Alekhya, and J. Seshadrinath, "Incipient inter-turn fault diagnosis in induction motors using CNN and LSTM based methods," in *2018 IEEE Industry Applications Society Annual Meeting (IAS)*, Sep. 2018, pp. 1–6, doi: 10.1109/IAS.2018.8544707.
- [37] S. Ray, B. Ganguly, and D. Dey, "Identification and classification of stator inter-turn faults in induction motor using wavelet kernel based convolutional neural network," *Electric Power Components and Systems*, vol. 48, no. 12–13, pp. 1421–1432, Aug. 2020, doi: 10.1080/15325008.2020.1854384.
- [38] M. H. Nazemi, D. Gallehdar, F. Haghjoo, and S. Cruz, "A secure and sensitive wavelet transform based technique for stator fault detection in the cases of line-connected and inverter-fed induction machines," *IET Electric Power Applications*, vol. 15, no. 9, pp. 1138–1153, Sep. 2021, doi: 10.1049/elp2.12084.
- [39] C.-Y. Lee and Y.-H. Cheng, "Motor fault detection using wavelet transform and improved PSO-BP neural network," *Processes*, vol. 8, no. 10, p. 1322, Oct. 2020, doi: 10.3390/pr8101322.
- [40] A. Almounajjed, A. K. Sahoo, M. K. Kumar, and S. K. Subudhi, "Stator fault diagnosis of induction motor based on discrete wavelet analysis and neural network technique," *Chinese Journal of Electrical Engineering*, vol. 9, no. 1, pp. 142–157, Mar. 2023, doi: 10.23919/CJEE.2023.000003.
- [41] Y. Xu, B. Klein, G. Li, and B. Gopaluni, "Evaluation of logistic regression and support vector machine approaches for XRF based particle sorting for a copper ore," *Minerals Engineering*, vol. 192, p. 108003, Feb. 2023, doi: 10.1016/j.mineng.2023.108003.
- [42] T. G. Dietterich and G. Bakiri, "Solving multiclass learning problems via error-correcting output codes," *Journal of Artificial Intelligence Research*, vol. 2, pp. 263–286, Jan. 1995, doi: 10.1613/jair.105.

## BIOGRAPHIES OF AUTHORS







**Partha Mishra**     is an assistant professor at College of Engineering and Management, Kolaghat, West Bengal, India. He received the B.E. degree in Electrical Engineering from the University of Burdwan in the year 2002, West Bengal, India, and the M.E degree in Electrical Engineering with specialization in High Voltage Engineering from Jadavpur University in the year 2009, West Bengal, India. His research areas are condition monitoring, signal processing, machine learning, deep learning, and statistical data analysis. He has published several research papers in the field of condition monitoring of induction motor. He can be contacted at email: parthaju2009@gmail.com.







**Shubhasish Sarkar**     received his B.Tech. degree (2005-2009) in Electrical Engineering from West Bengal University of Technology, India and M. E. degree (2009-2011) in High Voltage Engineering from Jadavpur University, India. Currently, he is pursuing his Ph.D. degree (registered in October 2020) in Electrical Engineering from Maulana Abul Kalam Azad University of Technology, India. From July 2011 to December 2017, he worked as an assistant professor in the Department of Electrical Engineering at Haldia Institute of Technology, West Bengal, India. From February 2018 onwards he is working as an assistant professor in the Electrical Engineering Department at Jalpaiguri Government Engineering College, West Bengal, India. His research interests include condition monitoring of induction motor, machine learning, and image/signal processing. He can be contacted at email: shubhasish.sarkar18@gmail.com.



**Dr. Sandip Saha Chowdhury**     is an associate professor in the Department of Electrical Engineering of Academy of Technology, Adisaptagram, West Bengal, India. He received the B.E.E, M.C.S.E and Ph.D. degree from Jadavpur University, West Bengal, India in 1999, 2002 and 2016, respectively. His research area of interests is numerical computation of electrostatic field. He can be contacted at email: sandipsahachowdhury@yahoo.co.in.



**Dr. Santanu Das**     received B.E.E and M.E.E degrees both from B.E. College (Deemed University), Shibpur, Howrah, India, and then, received Ph.D. in Electrical Engineering from Jadavpur University, Kolkata, India. He is currently working as a professor and head, Electrical Engineering Department, Jalpaiguri Government Engineering College, Jalpaiguri, India. He has published more than 70 research papers in reputed international journals and conferences. He has also authored one book for UG electrical engineering students. His current research interests include condition monitoring of electrical equipment, power quality event detection, signal processing, PLC based motion control, and power electronics and drives. He can be contacted at email: santanu.ddas@gmail.com.